



1

2

Carbon emission and export from Ket River, western Siberia

3

4

Artem G. Lim¹, Ivan V. Krickov¹, Sergey N. Vorobyev¹,

5

Mikhail A. Korets², Sergey Kopysov¹,

6

Liudmila S. Shirokova^{3,4}, Jan Karlsson⁵, and Oleg S. Pokrovsky^{3*}

7

¹*BIO-GEO-CLIM Laboratory, Tomsk State University, Tomsk, Russia*

8 ²*V.N. Sukachev Institute of Forest of the Siberian Branch of Russian Academy of Sciences – separated*
9 *department of the KSC SB RAS, Krasnoyarsk, 660036, Russia*

10 ³*Geosciences and Environment Toulouse, UMR 5563 CNRS, 14 Avenue Edouard Belin 31400 Toulouse,*
11 *France*

12 ⁴*N. Laverov Federal Center for Integrated Arctic Research, Russian Academy of Sciences, Arkhangelsk,*
13 *Russia*

14 ⁵*Climate Impacts Research Centre (CIRC), Department of Ecology and Environmental Science, Umeå*
15 *University, Linnaeus väg 6, 901 87 Umeå, Sweden.*

16

17
18 Key words: CO₂, C, emission, boreal, river, export, landscape, Siberia

19

20 * email: oleg.pokrovsky@get.omp.eu

21

22

23

24

25

26

27

28

29

30

31



32 **Abstract**

33 Despite recent progress in the understanding of the carbon (C) cycle of Siberian permafrost-affected
34 rivers, spatial and seasonal dynamics of C export and emission from medium-size rivers remain poorly
35 unknown. Here we studied one of the largest tributaries of the Ob River, the Ket River (watershed = 94,000
36 km²) which drains through virtually pristine dense taiga forest of the boreal zone in western Siberian Lowland
37 (WSL). We combined continuous in-situ measurements of carbon dioxide (CO₂) concentration and flux
38 (FCO₂), with methane (CH₄), organic and inorganic C (DOC and DIC, respectively), particulate organic C
39 and total bacterial concentrations over a 834-km transect of the Ket River main stem and its 26 tributaries
40 during spring flood and 12 tributaries during summer baseflow. The CO₂ concentration was lower and less
41 variable in the main stem (2000 to 2500 µatm) compared to that in tributaries (2000 to 5000 µatm). The
42 methane concentrations in the main stem and tributaries was a factor of 300 to 1900 (flood period) and 100
43 to 150 (baseflow period) lower than that of CO₂. The FCO₂ ranged from 0.4 to 2.4 g C m⁻² d⁻¹ in the main
44 channel and from 0.5 to 5.0 g C m⁻² d⁻¹ in the tributaries, being the highest during August in tributaries and
45 weakly dependent on season in the main channel. Only during summer baseflow, the DOM aromaticity,
46 bacterial number, and needleleaf forest coverage of the watershed positively affected CO₂ concentrations and
47 fluxes. We hypothesize that the relatively low variability in FCO₂ is due to flat homogeneous (bog and taiga
48 forest) landscape that results in long water residence times and stable input of allochthonous DOM, which
49 dominate the FCO₂. In summer baseflow, the DIC input from deeper flow paths might also contribute to CO₂
50 emission. The open water period (May to October) C emission from the Ket River basin was estimated to
51 127±11 Gg C y⁻¹ which is lower than the lateral C export during the same period. Although this estimated C
52 emissions contain uncertainties, stressing the need of better constrained FCO₂ and water coverage across
53 seasons, we considered it conservative which emphasize the important role of WSL rivers for release of CO₂
54 to the atmosphere.

55

56

57

58



59 **Introduction**

60 Assessment of greenhouse gas (GHG) emission from rivers is crucially important for understanding
61 the C cycle under various climate change scenarios (Campeau and del Giorgio, 2014; Chadburn et al., 2017;
62 Tranvik et al., 2018; Vonk et al., 2019; Vachon et al., 2020). Rivers receive terrestrial C and process and emit
63 a significant share of this C during transit to the sea (Liu et al., 2022). Quantifications of riverine C emissions
64 are sufficiently robust for relatively well studied regions of the world such as the European and N American
65 boreal zone (Dawson et al., 2004; Dinsmore et al., 2013; Wallin et al., 2013; Leith et al., 2015), or Arctic and
66 subarctic rivers of Alaska (Striegl et al., 2012; Crawford et al., 2013; Stackpoole et al., 2017). Despite
67 significant progress in assessing riverine pCO₂ in previously under-represented or ignored regions such as
68 lotic systems of Asia (Ran et al., 2015, 2017; Varol and Li, 2017) or South America (Almeida et al., 2017),
69 these studies generally use a combination of pH and alkalinity (DIC) to calculate the pCO₂ instead of direct
70 in-situ measurements, alike the studies of global emissions (Raymond et al., 2013; Lauerwald et al., 2015).
71 In this regard, regional high spatial resolution measurements of CO₂ concentration and fluxes of under-
72 represented regions are needed.

73 High latitude regions are important in this respect given their large C stocks, partly located in the
74 permafrost, and the observed and projected warming (Turetsky et al., 2020). This is especially true for Siberia,
75 hosting large C stocks in soils and wetlands intersected by extensive river networks that deliver majority of
76 water and C to the Arctic Ocean (Feng et al., 2013). There has been substantial progress in quantification of
77 carbon (C) transport and emissions from Siberian permafrost-affected rivers (Lobbés et al., 2000; Raymond
78 et al., 2007; Cooper et al., 2008; Semiletov et al., 2011; Feng et al., 2013; Griffin et al., 2018; Wild et al.,
79 2019). However, spatial and seasonal features of C export and emission from tributaries of Siberian rivers are
80 still remain poorly known. Existing data (Denfeld et al., 2013; Serikova et al., 2018; Karlsson et al., 2021;
81 Vorobyev et al., 2021) suggest that C (predominantly as CO₂) emissions from Siberian rivers can vary largely
82 over space and time. Such high variations do not allow reliable quantitative assessment of C emission and
83 integrating these values into regional and global C models.

84 In order to better understand and constrain the magnitude of C emission from Siberian rivers we
85 studied the Ket River (watershed 94,000 km²), a typical tributary of the Ob River in western Siberia. The Ob



86 river is the largest (in terms of watershed area) Siberian river and drains large pristine territories of taiga forest
87 and bogs. The catchment of Ob includes extensive regions of permafrost but a major part of it (80 %) is
88 situated in the permafrost-free zone of which very few data exist on riverine C emissions (Karlsson et al.,
89 2021). The Ket river drains permafrost-free western Siberian forest and wetlands with almost no human
90 activity, thus serving a representative system for understanding C cycling of permafrost-free rivers of an
91 underrepresented region of the world. We followed, via a boat routing over the main stem and main tributaries
92 of the river, the in-situ CO₂ concentrations combined with discrete regular sampling for dissolved CH₄, DOC,
93 DIC, total bacterial number and particulate organic matter. These measurements were complemented with
94 regular floating chamber measurements of CO₂ emission fluxes. We performed these observations during two
95 main open water seasons of the year - the peak of the spring flood and the end of the summer baseflow. Our
96 first objective was to quantify the difference in C concentration and emission during two seasons for the main
97 stem and the tributaries and to relate these differences to main physico-chemical parameters of the water
98 column and physio-geographical parameters (land cover) of the river watersheds. Our second objective was
99 to obtain total C emission flux from the river watershed area and compare it to lateral export yield of dissolved
100 and particulate carbon.

101

102 **2. Study Site, Materials and Methods**

103 *2.1. Ket River and its tributaries*

104 The Ket River main stem and its 26 tributaries sampled in this study include watersheds of distinct
105 sizes (catchment area ranged from 94,000 at the Ket's mouth to 20 km² of smallest tributary), but rather
106 similar lithology, climate and vegetation (**Fig. 1, Table S1**). This poorly accessible river basin is fully pristine
107 (50 % forest, 40 % wetlands), and has almost no agricultural and forestry activity. The watershed of Ket has
108 very low population density (0.27 person km⁻²) and lacks road infrastructure due to absence of hydrocarbon
109 exploration activity. In this regard, this river can serve as a model for medium size bog-forest rivers of the
110 western Siberia Lowland and results obtained from this watershed can be extrapolated to much larger
111 territory, comprising about 1 million km² of permafrost-free taiga forest and bog regions of the southern part
112 of WSL.



113 The mean annual air temperatures (MAAT) is $-0.6..-0.9$ °C and the mean annual precipitation is 520
114 mm y^{-1} in the central part of the basin. The lithology of this part of western Siberian lowland is dominated by
115 Pleistocene silts and sands with carbonate concretions overlaid by quaternary deposits (loesses, fluvial,
116 glacial and lacustrine deposits). The dominant soils are podzols in forest areas and histosols in peat bog
117 regions.

118 The peak of annual discharge in 2019 occurred in the end of May; in August, the discharge was 3 to
119 5 times smaller (**Fig. 1**). From May 18 to May 28, 2019, and from August 30 to September 2, 2019, we started
120 the boat trip in the middle course of the Ket River (Beliy Yar), and moved, first, 475 km upstream the Ket
121 river till its most headwaters, and then moved 834 km downstream till the river mouth, with an average speed
122 of 20 km h^{-1} . We stopped each 30-50 km along the Ket River and sampled for major hydrochemical
123 parameters, GHG, river suspended matter and total bacterial number of the main stem. We also moved several
124 km upstream of selected tributaries to record CO_2 concentrations for at least 1 h and to sample for river
125 hydrochemistry. At several occasions during spring flood, we monitored CO_2 concentration and performed
126 chamber measurements in the main stem and tributaries during both day and night time period.

127

128 2.2. CO_2 and CH_4 concentrations and CO_2 fluxes by floating chambers

129 Surface water CO_2 concentration was measured continuously, *in-situ* by deploying a portable infrared
130 gas analyzer (IRGA, GMT222 CARBOCAP® probe, Vaisala®; accuracy $\pm 1.5\%$) of two ranges (2 000 and
131 10 000 ppm) as described in previous work of our group on the Lena River (Vorobyev et al., 2021). The probe
132 was enclosed within a waterproof and gas-permeable membrane. For this, we used a protective expanded
133 polytetrafluoroethylene (PTFE) tube or sleeve that is highly permeable to CO_2 but impermeable to water
134 (Johnson et al., 2009). During the sampling, the sensor was left to equilibrate in the water for 10 minutes
135 before measurements were recorded. The sensor was placed into a tube which was submerged 0.5 m below
136 the water surface. A Campbell logger was connected to the system allowing continuous recording of the CO_2
137 concentration, water temperature and pressure every minute over 10 minute intervals yielding 732 individual
138 pCO_2 , water temperature and pressure values. The CO_2 concentrations in the Ket River tributaries included
139 between 10 and 20 individual pCO_2 readings for each tributary (250 measurements in total). In addition to



140 continuous *in-situ* CO₂ measurements, we estimated pCO₂ via measured pH and DIC values, using the set of
141 constants typically applied for riverine pCO₂ estimation in organic-rich waters (Cai and Wang, 1998;
142 DelDuco and Xu, 2017). The U-test (Mann-Whitney) demonstrated a lack of significant difference in CO₂
143 concentrations measured by Vaissala and calculated from the pH and DIC of the river water.

144 For CH₄ analyses, unfiltered water was sampled in 60-mL Serum bottles, closed without air bubbles
145 using vinyl stoppers and aluminum caps and immediately poisoned by adding 0.2 mL of saturated HgCl₂ via
146 a two-way needle system. Headspace was created in the laboratory and CH₄ concentrations were analyzed
147 using a Bruker GC-456 gas chromatograph (GC) equipped with flame ionization and thermal conductivity
148 detectors. Further details of CH₄ analyses are described elsewhere (Serikova et al., 2019; Vorobyev et al.,
149 2021).

150 The CO₂ fluxes were measured by using two floating CO₂ chambers equipped with non-dispersive
151 infrared SenseAir® CO₂ loggers (Bastviken et al., 2015), at each of the 7 (spring flood) and 6 (summer
152 baseflow) sampling location of the main stem and 26 tributaries following the procedures described elsewhere
153 (Serikova et al., 2019; Krickov et al., 2021). In addition to *in-situ* chamber measurements, the CO₂ flux was
154 calculated from measured CO₂ concentration using standard approaches (Guérin et al., 2007; Wanninkhof,
155 1992; Cole and Caraco, 1998). The value of K_T (gas transfer velocity) was calculated in two ways - assuming
156 zero wind speed and the actually measured wind speed at the site of sampling or at the nearest meteo-station
157 located in the Belyi Yar town, middle course of the Ket River. For comparison with previous estimates, we
158 also used a gas transfer velocity of 4.46 m d⁻¹ measured in the 4 largest rivers of Western Siberia Lowland
159 (WSL) in June 2015 (Ob', Pur, Pyakupur and Taz rivers, Karlsson et al., 2021) which is representative for
160 large lowland rivers (Alin et al., 2011; Beaulieu et al., 2012).

161

162 2.3. Chemical analyses of the river water

163 The dissolved oxygen (Cellox 325; accuracy of ±5%), specific conductivity (TetraCon 325; ±1.5%),
164 and water temperature (±0.2 °C) were measured *in-situ* at 20 cm depth using a WTW 3320 Multimeter. The
165 pH was measured using portable Hanna instrument via combined Schott glass electrode calibrated with NIST
166 buffer solutions (4.01, 6.86 and 9.18 at 25°C), with an uncertainty of 0.01 pH units. The temperature of buffer



167 solutions was within $\pm 2^{\circ}\text{C}$ of that of the river water. The water was sampled in pre-cleaned polypropylene
168 bottle from 20-30 cm depth in the middle of the river and immediately filtered through disposable single-use
169 sterile Sartorius filter units (0.45 μm pore size). The first 50 mL of filtrate was discarded. The DOC and
170 Dissolved Inorganic Carbon (DIC) were determined by a Shimadzu TOC-VSCN Analyzer (Kyoto, Japan)
171 with an uncertainty of 3% and a detection limit of 0.1 mg/L. Blanks of MilliQ water passed through the filters
172 demonstrated negligible release of DOC from the filter material. The SUVA was measured via ultraviolet
173 absorbance at 254 nm using a 10-mm quartz cuvette on a Bruker CARY-50 UV-VIS spectrophotometer.

174 The concentration of C and N in suspended material (Particulate Organic Carbon and Nitrogen (POC
175 and PON, respectively)) was determined via filtration of 1 to 2 L of freshly collected river water (at the river
176 bank or in the boat) with pre-weighted GFF filters (47 mm, 0.45 μm) and Nalgene 250-mL polystyrene
177 filtration units using a Mityvac® manual vacuum pump. Particulate C and N were measured using catalytic
178 combustion with Cu-O at 900°C with an uncertainty of $\leq 0.5\%$ using Thermo Flash 2000 CN Analyzer at
179 EcoLab, Toulouse. The samples were analyzed before and after 1:1 HCl treatment to distinguish between
180 total and inorganic C; however the ratio of $C_{\text{organic}} : C_{\text{carbonate}}$ in the river suspended matter (RSM) was always
181 above 20 and the contribution of carbonate C to total C in the RSM was equal in average $0.3 \pm 0.3\%$ (2 s.d., n
182 = 30).

183 Total microbial cell concentration was measured after sample fixation in glutaraldehyde, by a flow
184 cytometry (Guava® EasyCyte™ systems, Merck). Cells were stained using 1 μL of a 10 times diluted SYBR
185 GREEN solution (10000x, Merck), added to 250 μL of each sample before analysis. Particles were identified
186 as cells based on green fluorescence and forward scatter (Marie et al., 2001).

187

188 *2.5. Landscape parameters and water surface area of the Ket River basin*

189 The physio-geographical characteristics of the 26 Ket tributaries and the 7 points of the Ket main stem
190 (**Table S1, Fig. S1**) were determined by applying available digital elevation model (DEM GMTED2010),
191 soil, vegetation and lithological maps. The landscape parameters were typified using TerraNorte Database of
192 Land Cover of Russia (Bartalev et al., 2020; <http://terranorte.iki.rssi.ru>). This included various type of forest
193 (evergreen, deciduous, needleleaf/broadleaf), grassland, tundra, wetlands, water bodies and riparian zones.



194 The climate parameters the watershed were obtained from CRU grids data (1950-2016) (Harris et al., 2014)
195 and NCSCD data (Hugelius et al., 2013; [doi:10.5879/ecds/00000001](https://doi.org/10.5879/ecds/00000001)), respectively, whereas the biomass and
196 soil OC content were obtained from BIOMASAR2 (Santoro et al., 2010) and NCSCD databases. The
197 lithology layer was taken from GIS version of Geological map of the Russian Federation (scale 1 : 5 000 000,
198 <http://www.geolkarta.ru/>). We quantified river water surface area using the global SDG database with 30 m²
199 resolution (Pekel et al., 2016) including both seasonal and permanent water for the open water period of 2019
200 and for the multiannual average (reference period 2000-2004). We also used a more recent GRWL Mask
201 Database which incorporates first order wetted streams (Allen and Pavelsky, 2018).

202

203 *2.6. Data analysis*

204 Carbon concentrations and fluxes for all dataset were tested for normality using a Shapiro-Wilk test.
205 In case of the data were not normally distributed, we used non-parametric statistics. Comparisons of GHG
206 parameters in the main stem and tributaries during two sampling seasons were conducted using a non-
207 parametric Mann Whitney test at a significance level of 0.05. For comparison of unpaired data, a non-
208 parametric H-criterion Kruskal-Wallis test was used to reveal the differences between different study sites.
209 The Pearson rank order correlation coefficient ($p < 0.05$) was used to determine the relationship between CO₂
210 concentrations and emission fluxes and main landscape parameters of the Ket River tributaries, as well as
211 other potential drivers such as pH, O₂, water temperature, specific conductivity, DOC, DIC, particulate carbon
212 and nitrogen, and total bacterial number.

213

214 **3. Results**

215 *3.1. Greenhouse gases and dissolved and particulate C*

216 The main hydrochemical parameters and greenhouse gases concentration and emission fluxes of the
217 Ket River and its tributaries are listed in **Table 1** and primary data are provided in **Table S2** of the
218 Supplement. Continuous pCO₂ measurements in the main stem during the spring (764 individual data points
219 over the full distance of the boat route (834 km), demonstrated a lack of systematic change in CO₂
220 concentration from headwaters to the mouth. There were strong but non-systematic variations in CO₂



221 concentrations in the tributaries during the summer (**Fig. 2 A, B**). The CH₄ concentration (**Table 1 and Fig.**
222 **S2 A, B**) was low in the Ket River (around 0.17 and 0.86 μmol L⁻¹ in May and August, respectively) and in
223 the tributaries (range 0.09 to 2.57 μmol L⁻¹, 2 to 3 times higher values during the baseflow). These values are
224 consistent with the range of CH₄ concentration in other Siberian Rivers such as Lena (0.03 to 0.199 μmol L⁻¹
225 ¹, Bussman, 2013; Vorobyev et al., 2021). In the Ket River main stem and tributaries, the CH₄ concentrations
226 are 280-1900 and 100-154 times lower than those of CO₂ during spring and summer, respectively.
227 Consequently, diffuse CH₄ emissions (**Table 1, Fig. S2 C, D**) constituted 0.1 to 0.5% of total C emissions
228 and are not discussed in further detail.

229 During spring flood, CO₂ fluxes ranged from 0.26 to 3.2 g C m⁻² d⁻¹ in the main stem and tributaries
230 (**Table 1; Fig. 2 A**). During baseflow, the flux in the tributaries varied from 0.37 to 7.4 g C m⁻² d⁻¹ and was
231 a factor of 2 to 3 higher than that in the main stem (**Fig. 2 B, C, Table 1**). Note that peaks of CO₂ and CH₄
232 concentration at the main stem were not linked to conflux with tributaries. The CO₂ concentration in the river
233 water and gas transfer velocity assessed from discrete measurements by floating chambers ($K_T = 0.08$ - 1.83
234 m d⁻¹ in the main stem; 0.2 - 1.86 m d⁻¹ in the tributaries, **Table 1**) allowed for calculation of the continuous
235 CO₂ fluxes (**Fig. 2 A**). For this, we used an average value of k between two chamber sites (separated by a
236 distance of 50 to 100 km) to calculate the FCO₂ from in-situ measured pCO₂ in the river section between
237 these two sites.

238 The wind calculated flux was 1.2 to 2 times higher than that measured by chambers, whereas the
239 calculation with $K_T = 4.46$ m d⁻¹ overestimated the flux by a factor of 3.7 to 6.0. In both cases, the
240 overestimation of calculated flux relative to chamber-measured flux was most pronounced in the tributaries
241 rather than in the main stem. Overall, due to small size and short fetch of the Ket River and its tributaries, we
242 believe that lower values of K_T are more pertinent to the studied river basin. Given that the area is highly
243 flooded, this is consistent with observations in other flooded regions, where a canopy of vegetation protects
244 the water-air interface from wind stress thus rendering the gas transfer velocity lower compared to open water
245 such as large river (i.e., Foster-Martinez and Variano, 2016; Ho et al., 2018; Abril and Borges, 2019). We
246 therefore warn against the use of high value of transfer velocity, suitable for large rivers of the boreal zone,
247 for assessing the emissions in medium and small size, sheltered streams with extensive riparian vegetation.



248 The DIC concentration increased 5 to 10 times between the spring (2.4 to 2.8 mg L⁻¹) and summer
249 baseflow (18 to 20 mg L⁻¹) and the pH increased by 0.5-0.7 units between spring freshet and summer baseflow
250 (**Fig. 3** and **Fig. S3 A, B** of the Supplement). The DOC concentration ranged from 18 to 25 mg L⁻¹ during
251 flood and from 15 to 18 mg L⁻¹ during baseflow (**Fig. 3**). There was no systematic variations in DOC
252 concentration over the 834 km of the main stem (20.7 ± 3.6 and 15.0 ± 1.4 mg L⁻¹ in May and August,
253 respectively); however, it was slightly higher and more variable in the tributaries (22.0 ± 4.0 and 16.5 ± 7.4
254 mg L⁻¹, **Fig. S3 C, D**). The SUVA₂₅₄ remained highly stable throughout the seasons for both the tributaries
255 and the main stem (range from 4.2 to 4.9 L mg C⁻¹ m⁻¹, **Table 1**). The POC was 3 times higher during baseflow
256 compared to spring and ranged from 2 to 10 mg L⁻¹ (**Fig. 3** and **Fig. S3 E, F**). The total bacterial number
257 ranged from 5.0 × 10⁵ to 8.7 × 10⁵ cells mL⁻¹ for the main stem and tributaries without significant (p > 0.05)
258 seasonal variation (**Fig. 3** and **S3 G, H**).

259

260 3.2. Diurnal and spatial variation in CO₂ concentration and flux

261 The diel (day/night) measurements of CO₂ concentrations have been performed on six tributaries of
262 the Ket River during the spring flood period (**Fig. 4**). In two of them (Sochur ad Lopatka) we measured both
263 CO₂ concentration and CO₂ fluxes via floating chambers. Continuous CO₂ concentrations exhibited a
264 variation between 5 and 25% of the average value. Only in the case of a small tributary Segondenka (**Fig. 4**
265 **E**), when we measured CO₂ over 38 h, there was a local maximum in concentration between 6 and 7 pm
266 during the first and second day of monitoring, without any significant link to the water temperature. The
267 deviation of FCO₂ from the average value over the period of observation in two tributaries (**Fig. 4 A, B**) did
268 not exceed 20%, without any detectable difference between day and night period.

269 The spatial variation in pCO₂ and FCO₂ were tested during spring time in the flood zone of the Ket
270 River middle course, where the flood zone was connected to the main channel. Regardless of the distance
271 from the main stem and the size of the water body, the variation in pCO₂ and chamber-based fluxes were
272 within 30% of the values measured in the main stem. This suggests that the main stem parameters can be used
273 for upscaling the C emissions to the overall flood plain during May, provided that the water bodies are
274 connected to the rivers. Further test of spatial variation were performed on selected small tributaries, when



275 we moved 8 to 16 km upstream towards the headwaters and monitored the CO₂ concentration in the river
276 water. There was no sizable trend in CO₂ concentration over several km length of the tributary, consistent
277 with small fluctuations over the hundred km-scale of the main stem (**Fig. S4**). Altogether, rather minor spatial
278 and diel variations in both CO₂ concentration and emission fluxes support the chosen sampling strategy and
279 allow reliable extrapolation of obtained results to full surface of lotic waters of the Ket River basin, during
280 open water period.

281

282 *3.3. Impact of water chemistry and catchment characteristics on CO₂ concentration and flux*

283 There were generally no strong correlations between CO₂ and CH₄ and the main parameters of the
284 water column (DOC, DIC, POC, TBC and SUVA (**Table 2**)). The CO₂ concentration negatively correlated
285 with O₂ concentration ($R_{\text{Pearson}} = -0.68$, $p < 0.05$) and FCO₂ positively correlated with SUVA₂₅₄ ($R = 0.34$, p
286 < 0.05). Other hydro chemical characteristics of the water column did not impact CO₂ and CH₄ concentration
287 and CO₂ flux. During spring flood, there was no positive correlation between FCO₂ of the river water and
288 various hydrochemical characteristics. During the summer baseflow, there were positive correlations between
289 CO₂ concentration or flux and SUVA and total bacterial number (**Fig. 5 A, B**).

290 Among different landscape factors, only deciduous light needleleaf forest (larch trees) exhibited
291 significant ($p < 0.01$) positive correlations ($0.6 \leq R_s \leq 0.7$) with CO₂ concentration and flux of the Ket River
292 main stem and tributaries, detectable only during the summer baseflow period (**Fig. 5 C**). The peatland and
293 bogs at the watershed exhibited only weak, although positive ($0.2 < R_s < 0.4$), correlation with pCO₂ and
294 FCO₂ (**Fig. 5 D**). The other potentially important landscape factors of the river watershed (type of forest,
295 riparian and total aboveground vegetation, recent burns, water bodies) as well as lithological parameters
296 (clays, silts, sands with or without of the presence of carbonate concretions) did not significantly impact the
297 CO₂ and CH₄ concentration and measured CO₂ fluxes in the Ket River basin (**Table 2**). The mean annual
298 precipitation (MAP) at the watershed positively correlated with CO₂ and FCO₂ during the baseflow.

299

300

301



302 *3.4. Carbon emission and lateral export (yield) of the Ket River basin*

303 The C emissions (> 99.5 % CO₂, < 0.5 % CH₄) from the lotic waters of the Ket River basin were
304 assessed based on total river water coverage of the Ket watershed in 2019 (856 km², of which 691 km² is
305 seasonal water, according to the Global SDG database). Given that the measurements were performed at the
306 peak of spring flood in 2019, we used the maximal water coverage of the Ket River basin to calculate the
307 emissions during May and June, and baseflow measurements for July-October period.

308 For C emission calculation, we used the mean values of CO₂ emissions of the main stem and the
309 tributaries (1.31±0.81 g C m⁻² d⁻¹ for spring flood; 2.11±1.86 g C m⁻² d⁻¹ for summer-autumn baseflow) which
310 covers full variability of both tributaries and the Ket River main channel (**Table 1, Figure 3**). For the month
311 of July which was not sampled in this work and which represents a transition period between the flood and
312 the baseflow, we used the mean value of May and August (1.55 g C m⁻² d⁻¹). For the two months of maximal
313 water flow (May - June), the C emission from the whole Ket basin amounts to 68±42 Gg. When summed up
314 with July (25±20 Gg) and summer-autumn baseflow period (August to October) emission (32±28 Gg), the
315 total open water season emission flux is 127 Gg. The uncertainty on the total emission over 6 months of the
316 open water period is difficult to quantify but it can be estimated as between 30 and 50 %. This range covers
317 both the uncertainty of the water coverage of the territory and the seasonal and spatial variations of CO₂
318 emission in the Ket basin.

319 The C export flux (May to October) from the Ket basin was calculated based on monthly-averaged
320 discharge at the river mouth in 2019 available from Russian Hydrological Survey and DOC, DIC and POC
321 concentrations measured in the low reaches of the Ket River in this study (see hydrograph in **Fig. 1**). For this
322 calculation, we used DOC, DIC and POC concentrations measured during spring flood (for May and June
323 period) and baseflow (for August, September and October period). For the month of July, we used the mean
324 concentrations of end of May and August-September which is in accord with seasonal discharge pattern of
325 the Ket River. Note that the contribution of non-studied October month to total open water period water flux
326 is < 10 % and thus cannot provide sizable uncertainties. The total annual (excluding ice-covered period)
327 riverine C export from the Ket River basin ($S_{\text{watershed}} = 94,000 \text{ km}^2$) is 0.35 Tg (3.7 t C km⁻²_{land} y⁻¹), of which
328 DOC, DIC and POC accounts for 56, 24 and 20%, respectively. Therefore, over the 6 month of open water



329 period, the C emissions from lotic waters of Ket watershed constituted less than 30% of the dissolved and
330 particulate carbon lateral export from the river basin.

331

332

333 4. DISCUSSION

334 4.1. Temporal and spatial pattern of CO₂ emissions from the river waters

335 The first important result of the present study is quite low spatial and seasonal variability in both CO₂
336 concentration and emissions, as well as in DOC concentration and aromaticity (reflected by SUVA₂₅₄) in the
337 main channel (**Fig. 3, S3, Table 1**). The variability in the tributaries was much larger, with differences in
338 dissolved and gaseous C parameters between spring flood and summer-autumn baseflow (**Table S3**). While
339 CO₂ concentrations were different between tributaries and the main stem during both flood and baseflow, the
340 CO₂ flux was not different between the main stem and tributaries regardless of season (**Table S4**). This,
341 together with lack of diel variations in CO₂ concentrations and emissions during spring period of maximal
342 water coverage (**Fig. 4**) suggest rather stable pattern of CO₂ in the river water, not linked to short-scale
343 processes (primary productivity, photolysis, daily temperature variation). Indeed, negligible primary
344 productivity in the water column may stem from low water temperatures (9.3 °C), shallow photic layer of
345 organic-rich waters (DOC of 22 mg L⁻¹) and lack of periphyton activity during high flow of the spring flood.
346 Note that this finding contrasts the recent results of high frequency pCO₂ measurements in tropical and
347 temperate world rivers that show a 30 % higher nocturnal emission compared to daytime observations
348 (Gómez-Gener et al., 2021b).

349 Concerning spatial variability of C concentrations and emissions during the spring flood, the pCO₂
350 did not demonstrate sizable variation along the main stem of the Ket River and some of its tributaries, when
351 moving from the mouth to the headwaters. The SUVA also remained highly stable along the river flow. This,
352 together with a lack of pCO₂ or FCO₂ correlation with river watershed area during this period (**Table 2**)
353 suggest relatively modest control of headwater C cycling by ‘fresh’ unprocessed organic matter from upland
354 mire waters. Much stronger control of mire waters is reported in boreal zone of the Northern Europe (Wallin
355 et al., 2013, 2018). Furthermore, our results on the Ket River main stem and tributaries are in contrast to the



356 general view of disproportional importance of headwater streams in overall CO₂ emission from river basins
357 (Li et al., 2021). A likely explanation is relative low values of gas transfer velocity measured in the small
358 streams of the Ket basin in this study (0.2 - 2.0 m d⁻¹, **Table 1**). These values are typical of lakes rather than
359 rivers (i.e., Kokic et al., 2015) and stem from low flow rate, strongly forested and wind-protected river bed
360 without distinct valley due to generally flat orographic context of this part of the WSL (Serikova et al., 2018).

361 The second notable result is that, despite sizable variability of CO₂ in the tributaries, especially during
362 the baseflow, there were no correlations between either pCO₂ or FCO₂ and main hydrochemical parameters
363 of the water column (**Table 2**). We believe that main reasons of remarkable stability in CO₂ concentrations
364 and emissions and weak environmental control on dissolved and gaseous pattern in the Ket River basin are
365 (1) essentially homogeneous landscapes, lithology and quaternary deposits of the whole river basin (20-25 %
366 bogs, 60-70% forest, 3-5 % riparian zone), and (2) strong dominance of allochthonous sources in both
367 dissolved and particulate organic matter. Indeed, the SUVA and bacterial number (TBC) positively correlated
368 with both pCO₂ and FCO₂ during summer (**Fig. 5 A, B**), which may indicate non-negligible role of bacterial
369 processing of allochthonous (aromatic) DOC delivered to the water column from wetlands and mires.
370 Furthermore, the positive correlation between mean annual precipitation (MAP) and pCO₂ and FCO₂ during
371 the baseflow could reflect the importance of water storage in the mires and wetlands (which also showed
372 positive but less significant correlations, **Fig. 5 D**) during the summer time, and progressive release of CO₂
373 and DOC-rich waters from the wetlands to the streams. This terrestrial source could be either soil litter
374 leachates (in spring) or bog water (during baseflow, when the river water is substantially derived from
375 wetlands, Ala-aho et al., 2018a, b). Although we did not observe correlations between C emission and bog
376 coverage at the whole Ket River basin, it is known from works in boreal European zone that wetland streams
377 produce about twice higher CO₂ emission flux compared to forest streams (Gomez-Gener et al., 2021). The
378 patterns in CO₂ emissions observed in the present study during summer baseflow thus suggest the importance
379 of allochthonous organic matter from the peatland for CO₂ production in the water column and in soils where
380 the degradation of DOC is enhanced by the presence of bacteria.

381 Another interesting correlation is that between CO₂ flux during baseflow and the proportion of
382 deciduous needleleaf forest at the watershed (**Fig. 5 C**), which suggests the importance of C cycling by larch



383 trees and their possible control on the delivery of degradable organic matter to the river. Similar control of
384 larch vegetation on riverine CO₂ has been suggested for the Lena River, Eastern Siberia (Vorobyev et al.,
385 2021) although we acknowledge that further observations on contrasted Siberian watersheds are necessary to
386 confirm the observation that larch trees litterfall led to export of degradable OM to the river.

387 During both spring flood and summer baseflow, punctual local variations in CO₂ concentration and
388 emissions along the sampling route of the main stem (**Fig. 2 A**) were not necessarily linked to CO₂-rich
389 tributaries, or variations in water chemistry of the specific segments of the river. Similar to other studies of
390 boreal and subarctic rivers (i.e., Vorobyev et al., 2021; Lundin et al. 2013, Rocher-Ros et al. 2019), these
391 variations likely reflect local processes in the main stem, such as lateral influx from the shores and shallow
392 subsurface waters, sediment resuspension and respiration, or the discharge of underground, CO₂-rich fluids
393 in the river bed (hyporheic zone). Thus, via comprehensive analysis of 187 streams and rivers across the
394 contiguous United States, Hotchkiss et al. (2015) demonstrated that ~60% of CO₂ evasion is from external
395 sources rather than internal production. In view of lack of correlation of CO₂ emissions in the Ket River and
396 tributaries with hydrochemical parameters of the water column, we believe that external source of CO₂ in
397 studied river system represents sizable contribution to total riverine CO₂ evasion across the seasons and
398 sampling sites. In particular, in small peatland streams, the CO₂-rich deep peat/groundwater is known to be
399 the major source of aquatic CO₂ under low flow conditions (Dinsmore and Billett, 2008), whereas in boreal
400 headwater streams of N Sweden the main source of stream CO₂ was inflowing CO₂-rich soil waters
401 (Winterdahl et al., 2016).

402 At the Ket River basin, the local soil/groundwater effects are certainly more pronounced during
403 baseflow, due to lower impact of dilution, compared to the spring flood period. The hypothesis of deeper flow
404 path in summer compared to spring is confirmed for the WSL (Frey and McClelland, 2009; Pokrovsky et al.,
405 2015; Serikova et al., 2018) and is supported in this study by a strong increase in DIC concentration between
406 spring and summer (**Fig. 3**). Thus, although the pairwise correlations between parameters do not support any
407 particular mechanism, it is not excluded that OM bio- and photo degradation and local mire water feeding
408 drive FCO₂ in spring, and that deeper flowpaths and DIC export drive the elevated FCO₂ in summer.



409 Another important factor responsible for higher CO₂ production in the water column in summer
410 compared to spring could be POC degradation. The riverine POC is known to be more biodegradable than
411 DOC (Attermeyer et al., 2018), and the POC concentration in the Ket River basin increased 4-fold between
412 spring and summer (**Table 1**). The origin of summer-time POC and its lability remain elusive, but could be a
413 combination of plankton bloom and mire- or forest-derived DOC coagulation products in the water column
414 (Krickov et al., 2018). Furthermore, pronounced heterogeneity in CO₂ emission during baseflow among
415 tributaries may also reflect the heterogeneity of riverine organic matter which is known to be the maximal
416 during low flow conditions and minimal during high flow (Lynch et al., 2019).

417 Taken together, the present study demonstrates rather stable and non-equilibrium behavior of CO₂ in
418 the Ket River basin, with minimal role of *hot spots* from various local sources. In this regard, we note high
419 representability of studied riverine system for large pristine zones of taiga forest and bog regions of the WSL
420 - eastern smaller tributaries of the Ob River in permafrost-free zone (Chulym, Tym, Vakh, Agan, Trom'egan),
421 and also western tributaries of the Yenisey River (Dubches, Sym and Kas) with total watershed area of
422 350,000 km². To which degree the Ket River can serve as an analogue of another eastern tributary of the Ob
423 River, the more anthropogenically and agriculturally - impacted tributary Chulym River ($S_{\text{watershed}} = 134,000$
424 km²), remains unknown.

425

426 4.2. Emissions from the Ket River basin compared to lateral export of riverine carbon

427 The estimated C emissions (> 99.5 % C; < 0.5 % CH₄) from the Ket River main channel over 830 km
428 distance (0.5 to 2.5 g C m⁻² d⁻¹) are comparable to those of the Kolyma River (0.35 g C m⁻² d⁻¹ in the main
429 stem and 2.1 g C m⁻² d⁻¹ for lotic waters of the basin; Denfeld et al., 2013), the Ob River main channel
430 (1.32±0.14 g C m⁻² d⁻¹ in the permafrost-free zone; Karlsson et al., 2021), and the Lena River (0.8 to 1.7 g C
431 m⁻² d⁻¹; Vorobyev et al., 2021). The CO₂ emission in Ket's tributaries (1 to 2 g C m⁻² d⁻¹ in spring; 1 to 5 g C
432 m⁻² d⁻¹ in summer) are within the range reported for small rivers and streams of the permafrost-free zone of
433 western Siberia (0 to 3.6 g C m⁻² d⁻¹ in spring; 4 to 9 g C m⁻² d⁻¹ in summer; Serikova et al., 2018), forest and
434 wetland headwater streams of northern Sweden (0.5 to 5 g C m⁻² d⁻¹; Gomez-Gener et al., 2021), rivers and
435 headwater streams of the Unites States (2.7 to 3.1 g C m⁻² d⁻¹, Butman and Raymond, 2011; Hotchkiss et al.,



436 2015), small mountain streams in Northern Europe ($3.3 \text{ g C m}^{-2} \text{ d}^{-1}$, Rocher-Ros et al., 2019), boreal streams
437 in Canada and Alaska (0.8 to $5.2 \text{ g C m}^{-2} \text{ d}^{-1}$, Koprivnjak et al., 2010; Teodoru et al., 2009; Crawford et al.,
438 2013; Campeau et al., 2014).

439 Total C emissions from the water surfaces of the Ket River basin assessed in this study (148 g C-CO_2
440 $\text{m}^{-2} \text{ y}^{-1}$, assuming no emission under ice) are lower than those of the lotic waters of western Siberia (898 g C-
441 $\text{CO}_2 \text{ m}^{-2} \text{ y}^{-1}$, Karlsson et al., 2021) but comparable to global C emissions from the Lena river basin (180 to
442 $360 \text{ g C m}^{-2} \text{ y}^{-1}$, Vorobyev et al., 2021). When normalized to the Ket river basin area ($S_{\text{watershed}} = 94,000 \text{ km}^2$),
443 the C emission amounts to $1.35 \text{ g C m}^{-2}_{\text{land}} \text{ y}^{-1}$. Hutchins et al. (2020) reported 0.63 to $0.29 \text{ g C-CO}_2 \text{ m}^{-2}_{\text{land}} \text{ y}^{-1}$
444 emission from 50 small streams in boreal biome of Canada, comparable to the headwater stream network
445 emissions in Alaska ($0.44 \text{ g C m}^{-2} \text{ y}^{-1}$, Crawford et al., 2013) and Zolkos et al. (2019) found approximately
446 $0.4 \text{ g C m}^{-2} \text{ y}^{-1}$ in the Northwest Territories. Much higher land area - specific emissions, comparable or
447 exceeding those of the Ket River, were reported in Québec (1.0 to $4.6 \text{ g C m}^{-2} \text{ y}^{-1}$; Campeau and del Giorgio,
448 2014; Hutchins et al., 2019; Teodoru et al., 2009), Sweden (1.6 to $8.6 \text{ g C m}^{-2} \text{ y}^{-1}$; Humborg et al., 2010;
449 Jonsson et al., 2007; Lundin et al., 2013; Wallin et al., 2011, 2018) and boreal portions of the Yukon River
450 (7 to $9 \text{ g C m}^{-2} \text{ y}^{-1}$; Striegl et al., 2012; Stackpoole et al., 2017). Possible reasons for these differences could
451 be different areal coverage of the territory by river network, the calculated rather than measured CO_2 fluxes,
452 or the higher gas transfer velocity in the rivers from mountainous regions.

453 The regional assessment of the Ket River basin performed in this study are based on direct chamber
454 measurements of emissions and as such provide rigorous basis for upscaling the CO_2 emissions from currently
455 understudied lotic waters of permafrost-free zone of Western Siberia. The C evasion from the Ket basin
456 assessed in the present work ($127 \pm 11 \text{ Gg y}^{-1}$, ignoring the emission during the ice breakup in early spring)
457 is 3 times lower than the total (DOC+DIC+POC) lateral export by this river from the same territory (0.35 Tg
458 C y^{-1}). The lateral C loss (yield) for the Ket River ($3.7 \text{ t C km}^{-2}_{\text{land}} \text{ y}^{-1}$) is in agreement with regional C
459 (DOC+DIC) yield by permafrost-free small and medium size rivers of the WSL (3 to $4 \text{ t C km}^{-2}_{\text{land}} \text{ y}^{-1}$,
460 Pokrovsky et al., 2020) and with the Ob River in its the middle course at the latitude of the Ket River (3.6 t
461 $\text{C km}^{-2}_{\text{land}} \text{ y}^{-1}$, Vorobyev et al., 2019). Such high C yields in the southern, permafrost-free part of the WSL
462 stem from essentially inorganic carbon originated from groundwater discharge of carbonate mineral rich



463 reservoirs, abundant in this region (Pokrovsky et al., 2015). At the same time, the organic C yield in rivers of
464 this region is quite low and represents less than 20% of total C yield (Pokrovsky et al., 2020; Vorobyev et al.,
465 2019). This can explain anomalously low value of C evasion : C export of the Ket River (1 : 3) measured in
466 this work as compared to the average values for permafrost-free zone of Western Siberia (1 : 1, Serikova et
467 al., 2019). One should also note that the gas transfer velocity measured in thus study provides much lower
468 fluxes than those calculated with $K_T = 4.46 \text{ m d}^{-1}$ in previous studies (**Table S2**). Another factors potentially
469 leading to underestimation of C evasion in this study is GIS-based minimal water coverage which does not
470 include seasonal oxbow lakes, flooded forest and temporary water bodies of the floodplain which provide
471 sizable emissions (see Krickov et al., 2021). We also do not exclude that some important hot moments / hot
472 spots of C emission were missed in our sampling campaign, such as summer baseflow/autumn peaks
473 (Serikova et al., 2019) or stagnant zones of the floodplain in summer (Krickov et al., 2021; Castro-Morales
474 et al., 2021). This calls a need for higher spatial and temporal resolution monitoring of C emission, with
475 special focus on important events across full hydrological continuum.

476

477 **5. Concluding remarks**

478 Via combination of discrete floating chamber and hydrochemistry and continuous CO_2 concentration
479 measurements over 830 km of large pristine boreal river of western Siberia main channel and its 26 tributaries
480 during the peak of spring flood and the summer-autumn baseflow, we quantified spatial and temporal
481 variations, overall emissions of C (CO_2 , CH_4) and export of (DOC, DIC and POC) during the 6 months of
482 open water period. The range of CO_2 and CH_4 concentrations in the main channel and tributaries as well as
483 CO_2 emissions were consistent with other boreal and subarctic regions but demonstrated rather low seasonal
484 and spatial variability. The diel CO_2 flux by floating chambers and continuous pCO_2 measurements in the
485 tributaries of the Ket River during spring flood demonstrated negligible impact of day/night period on the
486 CO_2 concentrations and emission fluxes. During spring flood, there were no correlations between
487 concentrations of CO_2 and CH_4 , or CO_2 flux and their main potential controlling physiochemical parameters
488 of the water column as well as climatic and landscape parameters of the watershed.



489 We hypothesize that homogeneous landscape coverage (bog and taiga forest) provide stable
490 allochthonous input of DOM as confirmed by very weak spatial and seasonal variations of DOM aromaticity.
491 Among possible driving factors of CO₂ production in the water column (bio- and photo-degradation of DOC
492 and POC, plankton metabolism), none seems to be sizably important for persistent CO₂ supersaturation and
493 relevant emissions. The landscape factors of the watershed (bog and forest coverage, soil organic carbon
494 stock) of the tributaries and along the main stem did not sizably affected the C concentration and emission
495 pattern across two seasons. We hypothesize that stable terrestrial input of strongly aromatic DOM, shallow
496 photic layer and humic waters of the Ket River basin preclude sizable daily and seasonal variations of C
497 parameters. Punctual discharge of groundwaters, resuspension of sediments or shallow subsurface influx from
498 mires and riparian zone may be responsible for small-scale heterogeneities in C emissions and concentrations
499 along the main stem and among the tributaries. These effects are much stronger pronounced during summer
500 baseflow compared to spring flood. Overall, deeper flow paths in summer compared to spring enhance the
501 DIC discharge within the river bed and the tributaries, thus leading to elevated CO₂ flux in summer.
502 Additional factor responsible for higher CO₂ emission during this season could be mire-originated particulate
503 organic matter (POM) processing in the water column. Further experiments on POM degradation and isotope
504 tracing of C sources are therefore needed to quantitatively discriminate between surficial “organic” and deep
505 “inorganic” source of CO₂ in the Ket River basin during summer baseflow. In this regard, a reason for
506 relatively low spatial and temporal variability of CO₂ concentration and emissions in this large river basin
507 could be that existing variations in C supply and control of FCO₂ are coupled and counteract each other so
508 that the net FCO₂ remains spatially and temporally stable.

509 The six month open-water period C emissions from the lotic waters of the Ket River basin were sizably
510 lower than the lateral C export by this river during the same period. We conclude that regional estimations
511 of C balance in lotic systems should be based on a combination of direct chamber measurements, discrete
512 hydrochemical sampling and continuous in-situ monitoring with submersible sensors, at least during two most
513 important hydrological periods of the year which are, for boreal regions, the spring flood and the summer-
514 autumn baseflow. We believe that this is the best trade-off between scientific rigor and logistical feasibility
515 in poorly accessible, pristine and strongly understudied regions.



516

517 **Acknowledgements.**

518 We acknowledge support from RSF grant 22-17-00253, RFBR grant 20-05-00729, the TSU Development
519 Program “Priority-2030”, grant “Kolmogorov” of MES (Agreement No 075-15-2022-241), and the Swedish
520 Research Council (grant no. 2016-05275).

521

522 **Authors contribution.**

523 AL and OP designed the study and wrote the paper; AL, SV, IK and OP performed sampling, analysis and
524 their interpretation; LS performed bacterial assessment and DOC/DIC analysis and interpretation; MK
525 performed landscape characterization of the Ket River basin and calculated water surface area; SK
526 performed hydrological analysis; JK provided analyses of literature data, transfer coefficients for FCO₂
527 calculations and global estimations of areal emission vs export.

528

529 **Competing interests.**

530 The authors declare that they have no conflict of interest.

531

532 **References**

- 533 Abril, G. and Borges, A. V.: Ideas and perspectives: Carbon leaks from flooded land: do we need to replumb
534 the inland water active pipe? *Biogeosciences*, 16, 769–784, <https://doi.org/10.5194/bg-16-769-2019>,
535 2019.
- 536 Ala-Aho, P., Soulsby, C., Pokrovsky, O. S., Kirpotin, S. N., Karlsson, J., Serikova, S., Manasypov, R., Lim,
537 A., Krickov, I., Kolesnichenko, L. G., Laudon, H., and Tetzlaff, D.: Permafrost and lakes control river
538 isotope composition across a boreal Arctic transect in the Western Siberian lowlands, *Environ. Res.*
539 *Let.*, 13, <https://doi.org/10.1088/1748-9326/aaa4fe>, 2018a.
- 540 Ala-aho, P., Soulsby, C., Pokrovsky, O. S., Kirpotin, S. N., Karlsson, J., Serikova, S., Vorobyev, S. N.,
541 Manasypov, R. M., Loiko, S., and Tetzlaff, D.: Using stable isotopes to assess surface water source
542 dynamics and hydrological connectivity in a high-latitude wetland and permafrost influenced
543 landscape, *J. Hydrol.*, 556, 279–293, <https://doi.org/10.1016/j.jhydrol.2017.11.024>, 2018b.
- 544 Alin, S. R., Rasera, M. D. F. F. L., Salimon, C. I., Richey, J. E., Holtgrieve, G. W., Krusche, A. V., and
545 Snidvongs, A.: Physical controls on carbon dioxide transfer velocity and flux in low-gradient river
546 systems and implications for regional carbon budgets, *J. Geophys. Res. Biogeosciences*, 116,
547 <https://doi.org/10.1029/2010JG001398>, 2011.
- 548 Allen, G. H. and Pavelsky, T. M.: Global extent of rivers and streams, *Science*, 361, 585–588,
549 <https://doi.org/10.1126/science.aat0636>, 2018.
- 550 Almeida, R. M., Pacheco, F. S., Barros, N., Rosi, E., and Roland, F.: Extreme floods increase CO₂ outgassing
551 from a large Amazonian rive, *Limnol. Oceanogr.*, 62, 989–999, <https://doi.org/10.1002/lno.10480>,
552 2017.
- 553 Attermeyer, K., Catalán, N., Einarsdottir, K., Freixa, A., Groeneveld, M., Hawkes, J. A., Bergquist, J., and
554 Tranvik, L. J.: Organic carbon processing during transport through boreal inland waters: particles as
555 important sites, *J. Geophys. Res. Biogeosciences*, 123, 2412–2428,
556 <https://doi.org/10.1029/2018JG004500>, 2018.



- 557 Bartalev, S. A., Egorov, V. A., Ershov, D. V., Isaev, A. S., Lupyan, E. A., Plotnikov, D. E., and Uvarov, I.
558 A.: Remote mapping of vegetation land cover of Russia based on data of MODIS spectroradiometer,
559 *Mod. Probl. Earth Remote Sens. Space*, 8, 285–302, 2018.
- 560 Bastviken, D., Sundgren, I., Natchimuthu, S., Reyier, H., and Gålfalk, M.: Technical Note: Cost-efficient
561 approaches to measure carbon dioxide (CO₂) fluxes and concentrations in terrestrial and aquatic
562 environments using mini loggers, *Biogeosciences*, 12, 3849–3859, [https://doi.org/10.5194/bg-12-3849-](https://doi.org/10.5194/bg-12-3849-2015)
563 2015, 2015.
- 564 Beaulieu, J. J., Shuster, W. D., and Rebholz, J. A.: Controls on gas transfer velocities in a large river, *J.*
565 *Geophys. Res. Biogeosciences*, 117, G02007, <https://doi.org/10.1029/2011JG001794>, 2012.
- 566 Bussmann, I.: Distribution of methane in the Lena Delta and Buor-Khaya Bay, Russia, *Biogeosciences*, 10,
567 4641–4652, <https://doi.org/10.5194/bg-10-4641-2013>, 2013.
- 568 Butman, D. and Raymond, P. A.: Significant efflux of carbon dioxide from streams and rivers in the United
569 States, *Nat. Geosci.*, 4, 839–842, <https://doi.org/10.1038/ngeo1294>, 2011.
- 570 Cai, W.-J. and Wang, Y.: The chemistry, fluxes, and sources of carbon dioxide in the estuarine waters of the
571 Satilla and Altamaha Rivers, Georgia, *Limnol. Oceanogr.*, 43, 657–668,
572 <https://doi.org/10.4319/lo.1998.43.4.0657>, 1998.
- 573 Campeau, A. and del Giorgio, P. A.: Patterns in CH₄ and CO₂ concentrations across boreal rivers: Major
574 drivers and implications for fluvial greenhouse emissions under climate change scenarios, *Glob.*
575 *Change Biol.*, 20, 1075–1088, <https://doi.org/10.1111/gcb.12479>, 2014.
- 576 Campeau, A., Lapierre, J.-F., Vachon, D., and del Giorgio, P. A.: Regional contribution of CO₂ and CH₄
577 fluxes from the fluvial network in a lowland boreal landscape of Québec, *Glob. Biogeochem. Cycles*,
578 28, 57–69, <https://doi.org/10.1002/2013GB004685>, 2014.
- 579 Castro-Morales, K., Canning, A., Körtzinger, A., Göckede, M., Küsel, K., Overholt, W. A., Wichard, T.,
580 Redlich, S., Arzberger, S., Kolle, O., and Zimov, N.: Effects of reversal of water flow in an Arctic
581 floodplain river on fluvial emissions of CO₂ and CH₄, *J. Geophys. Res. Biogeosciences*, 127,
582 e2021JG006485, <https://doi.org/10.1029/2021JG006485>, 2022.
- 583 Chadburn, S. E., Krinner, G., Porada, P., Bartsch, A., Beer, C., Beelli Marchesini, L., Boike, J., Ekici, A.,
584 Elberling, B., Friborg, T., Hugelius, G., Johansson, M., Kuhry, P., Kutzbach, L., Langer, M., Lund, M.,
585 Parmentier, F.-J. W., Peng, S., Van Huissteden, K., Wang, T., Westermann, S., Zhu, D., and Burke, E.
586 J.: Carbon stocks and fluxes in the high latitudes: using site-level data to evaluate Earth system models,
587 *Biogeosciences*, 14, 5143–5169, <https://doi.org/10.5194/bg-14-5143-2017>, 2017.
- 588 Cole, J. J. and Caraco, N. F.: Atmospheric exchange of carbon dioxide in a low-wind oligotrophic lake
589 measured by the addition of SF₆, *Limnol. Oceanogr.*, 43, 647–656,
590 <https://doi.org/10.4319/lo.1998.43.4.0647>, 1998.
- 591 Cooper, L. W., McClelland, J. W., Holmes, R. M., Raymond, P. A., Gibson, J. J., Guay, C. K., and Peterson,
592 B. J.: Flow-weighted values of runoff tracers ($\delta^{18}\text{O}$, DOC, Ba, alkalinity) from the six largest Arctic
593 rivers, *Geophys. Res. Lett.*, 35, L18606, <https://doi.org/10.1029/2008GL035007>, 2008.
- 594 Crawford, J. T., Striegl, R. G., Wickland, K. P., Dornblaser, M. M., and Stanley, E. H.: Emissions of carbon
595 dioxide and methane from a headwater stream network of interior Alaska, *J. Geophys. Res.*
596 *Biogeosciences*, 118, 482–494, <https://doi.org/10.1002/jgrg.20034>, 2013.
- 597 Crawford, J. T., Loken, L. C., Casson, N. J., Smith, C., Stone, A. G., and Winslow, L. A.: High-speed
598 limnology: using advanced sensors to investigate spatial variability in biogeochemistry and hydrology,
599 *Environ. Sci. Technol.*, 49, 442–450, <https://doi.org/10.1021/es504773x>, 2015.
- 600 Dawson, J. J., Billett, M. F., Hope, D., Palmer, S. M., and Deacon, C.: Sources and sinks of aquatic carbon
601 in a peatland stream continuum, *Biogeochemistry*, 70, 71–92, 2004.
- 602 DelDuco, E. M. and Xu, Y. J.: Dissolved carbon transport and processing in North America’s largest swamp
603 river entering the Northern Gulf of Mexico, *Water*, 11, 1395, <https://doi.org/10.3390/w11071395>, 2019.
- 604 Denfeld, B. A., Frey, K. E., Sobczak, W. V., Mann, P. J., and Holmes, R. M.: Summer CO₂ evasion from
605 streams and rivers in the Kolyma River basin, north-east Siberia, *Polar Res.*, 32, 19704,
606 <https://doi.org/10.3402/polar.v32i0.19704>, 2013.
- 607 Dinsmore, K. J. and Billett, M. F.: Continuous measurement and modeling of CO₂ losses from a peatland
608 stream during stormflow events, *Water Resour. Res.*, 44, W12417,
609 <https://doi.org/10.1029/2008WR007284>, 2008.



- 610 Dinsmore, K. J., Billett, M. F., and Dyson, K. E.: Temperature and precipitation drive temporal variability in
611 aquatic carbon and GHG concentrations and fluxes in a peatland catchment, *Glob. Change Biol.*, 19,
612 2133–2148, <https://doi.org/10.1111/gcb.12209>, 2013.
- 613 Feng, X., Vonk, J. E., Dongen, B. E. V., Gustafsson, Ö., Semiletov, I. P., Dudarev, O. V., Wang, Z.,
614 Montluçon, D. B., Wacker, L., and Eglinton, T. I.: Differential mobilization of terrestrial carbon pools
615 in Eurasian Arctic river basins, *Proc. Natl. Acad. Sci. U. S. A.*, 110, 14168–14173,
616 <https://doi.org/10.1073/pnas.1307031110>, 2013.
- 617 Foster-Martinez, M. R. and Variano, E. A.: Air-water gas exchange by waving vegetation stems, *J. Geophys.*
618 *Res. Biogeosciences*, 121, 1916–1923, <https://doi.org/10.1002/2016JG003366>, 2016.
- 619 Frey, K. E. and McClelland, J. W.: Impacts of permafrost degradation on arctic river biogeochemistry,
620 *Hydrol. Process.*, 23, 169–182, <https://doi.org/10.1002/hyp.7196>, 2009.
- 621 Gómez-Gener, L., Rocher-Ros, G., Battin, T., Cohen, M. J., Dalmagro, H. J., Dinsmore, K. J., Drake, T. W.,
622 Duvert, C., Enrich-Prast, A., Horgby, Å., Johnson, M. S., Kirk, L., Machado-Silva, F., Marzolf, N. S.,
623 McDowell, M. J., McDowell, W. H., Miettinen, H., Ojala, A. K., Peter, H., Pumpanen, J., Ran, L.,
624 Riveros-Iregui, D. A., Santos, I. R., Six, J., Stanley, E. H., Wallin, M. B., White, S. A., and Sponseller,
625 R. A.: Global carbon dioxide efflux from rivers enhanced by high nocturnal emissions, *Nat. Geosci.*,
626 1–6, <https://doi.org/10.1038/s41561-021-00722-3>, 2021a.
- 627 Gómez-Gener, L., Hotchkiss, E. R., Laudon, H., and Sponseller, R. A.: Integrating discharge-concentration
628 dynamics across carbon forms in a boreal landscape, *Water Resour. Res.*, 57, e2020WR028806,
629 <https://doi.org/10.1029/2020WR028806>, 2021b.
- 630 Griffin, C. G., McClelland, J. W., Frey, K. E., Fiske, G., and Holmes, R. M.: Quantifying CDOM and DOC
631 in major Arctic rivers during ice-free conditions using Landsat TM and ETM+ data, *Remote Sens.*
632 *Environ.*, 209, 395–409, <https://doi.org/10.1016/j.rse.2018.02.060>, 2018.
- 633 Guérin, F., Abril, G., Serça, D., Delon, C., Richard, S., Delmas, R., Tremblay, A., and Varfalvy, L.: Gas
634 transfer velocities of CO₂ and CH₄ in a tropical reservoir and its river downstream, *J. Mar. Syst.*, 66,
635 161–172, <https://doi.org/10.1016/j.jmarsys.2006.03.019>, 2007.
- 636 Harris, I., Jones, P. d., Osborn, T. j., and Lister, D. h.: Updated high-resolution grids of monthly climatic
637 observations – the CRU TS3.10 Dataset, *Int. J. Climatol.*, 34, 623–642,
638 <https://doi.org/10.1002/joc.3711>, 2014.
- 639 Ho, D. T., Engel, V. C., Ferrón, S., Hickman, B., Choi, J., and Harvey, J. W.: On factors influencing air-water
640 gas exchange in emergent wetlands, *J. Geophys. Res. Biogeosciences*, 123, 178–192,
641 <https://doi.org/10.1002/2017JG004299>, 2018.
- 642 Holmes, R. M., Coe, M. T., Fiske, G. J., Gurtovaya, T., McClelland, J. W., Shiklomanov, A. I., Spencer, R.
643 G. M., Tank, S. E., and Zhulidov, A. V.: Climate change impacts on the hydrology and biogeochemistry
644 of Arctic Rivers, in: *Climatic Changes and Global warming of Inland Waters: Impacts and Mitigation*
645 *for Ecosystems and Societies*, edited by: Goldman, C. R., Kumagi, M., and Robarts, R. D., John Wiley
646 and Sons, 1–26, 2013.
- 647 Hotchkiss, E. R., Hall Jr, R. O., Sponseller, R. A., Butman, D., Klaminder, J., Laudon, H., Rosvall, M., and
648 Karlsson, J.: Sources of and processes controlling CO₂ emissions change with the size of streams and
649 rivers, *Nat. Geosci.*, 8, 696–699, <https://doi.org/10.1038/ngeo2507>, 2015.
- 650 Hugelius, G., Tamocai, C., Broll, G., Canadell, J. G., Kuhry, P., and Swanson, D. K.: The northern
651 circumpolar soil carbon database: Spatially distributed datasets of soil coverage and soil carbon storage
652 in the northern permafrost regions, *Earth Syst. Sci. Data*, 5, 3–13, [https://doi.org/10.5194/essd-5-3-](https://doi.org/10.5194/essd-5-3-2013)
653 2013, 2013.
- 654 Humborg, C., Mörth, C.-M., Sundbom, M., Borg, H., Blenckner, T., Giesler, R., and Ittekkot, V.: CO₂
655 supersaturation along the aquatic conduit in Swedish watersheds as constrained by terrestrial
656 respiration, aquatic respiration and weathering, *Glob. Change Biol.*, 16, 1966–1978,
657 <https://doi.org/10.1111/j.1365-2486.2009.02092.x>, 2010.
- 658 Hutchins, R. H. S., Prairie, Y. T., and del Giorgio, P. A.: Large-Scale Landscape Drivers of CO₂, CH₄, DOC,
659 and DIC in Boreal River Networks, *Glob. Biogeochem. Cycles*, 33, 125–142,
660 <https://doi.org/10.1029/2018GB006106>, 2019.
- 661 Hutchins, R. H. S., Tank, S. E., Olefeldt, D., Quanton, W. L., Spence, C., Dion, N., Estop-Aragonés, C., and
662 Mengistu, S. G.: Fluvial CO₂ and CH₄ patterns across wildfire-disturbed ecozones of subarctic Canada:



- 663 Current status and implications for future change, *Glob. Change Biol.*, 26, 2304–2319,
664 <https://doi.org/10.1111/gcb.14960>, 2020.
- 665 Johnson, M. S., Billett, M. F., Dinsmore, K. J., Wallin, M., Dyson, K. E., and Jassal, R. S.: Direct and
666 continuous measurement of dissolved carbon dioxide in freshwater aquatic systems—method and
667 applications, *Ecohydrology*, 3, 68–78, <https://doi.org/10.1002/eco.95>, 2009.
- 668 Jonsson, A., Algesten, G., Bergström, A.-K., Bishop, K., Sobek, S., Tranvik, L. J., and Jansson, M.:
669 Integrating aquatic carbon fluxes in a boreal catchment carbon budget, *J. Hydrol.*, 334, 141–150,
670 <https://doi.org/10.1016/j.jhydrol.2006.10.003>, 2007.
- 671 Karlsson, J., Serikova, S., Vorobyev, S. N., Rocher-Ros, G., Denfeld, B., and Pokrovsky, O. S.: Carbon
672 emission from Western Siberian inland waters, *Nat. Commun.*, 12, 825, <https://doi.org/10.1038/s41467-021-21054-1>, 2021.
- 674 Kokic, J., Wallin, M. B., Chmiel, H. E., Denfeld, B. A., and Sobek, S.: Carbon dioxide evasion from
675 headwater systems strongly contributes to the total export of carbon from a small boreal lake catchment,
676 *J. Geophys. Res. Biogeosciences*, 120, 13–28, <https://doi.org/10.1002/2014JG002706>, 2015.
- 677 Koprivnjak, J.-F., Dillon, P. J., and Molot, L. A.: Importance of CO₂ evasion from small boreal streams, *Glob.*
678 *Biogeochem. Cycles*, 24, GB4003, <https://doi.org/10.1029/2009GB003723>, 2010.
- 679 Krickov, I. V., Lim, A. G., Manasypov, R. M., Loiko, S. V., Shirokova, L. S., Kirpotin, S. N., Karlsson, J.,
680 and Pokrovsky, O. S.: Riverine particulate C and N generated at the permafrost thaw front: Case study
681 of western Siberian rivers across a 1700 km latitudinal transect, *Biogeosciences*, 6867–6884,
682 <https://doi.org/10.5194/bg-15-6867-2018>, 2018.
- 683 Krickov, I. V., Serikova, S., Pokrovsky, O. S., Vorobyev, S. N., Lim, A. G., Siewert, M. B., and Karlsson, J.:
684 Sizable carbon emission from the floodplain of Ob River, *Ecol. Indic.*, 131, 108164,
685 <https://doi.org/10.1016/j.ecolind.2021.108164>, 2021.
- 686 Lauerwald, R., Laruelle, G. G., Hartmann, J., Ciais, P., and Regnier, P. A. G.: Spatial patterns in CO₂ evasion
687 from the global river network, *Glob. Biogeochem. Cycles*, 29, 534–554,
688 <https://doi.org/10.1002/2014GB004941>, 2015.
- 689 Leith, F. I., Dinsmore, K. J., Wallin, M. B., Billett, M. F., Heal, K. V., Laudon, H., Öquist, M. G., and Bishop,
690 K.: Carbon dioxide transport across the hillslope–riparian–stream continuum in a boreal headwater
691 catchment, *Biogeosciences*, 12, 1881–1892, <https://doi.org/10.5194/bg-12-1881-2015>, 2015.
- 692 Li, M., Peng, C., Zhang, K., Xu, L., Wang, J., Yang, Y., Li, P., Liu, Z., and He, N.: Headwater stream
693 ecosystem: an important source of greenhouse gases to the atmosphere, *Water Res.*, 190, 116738,
694 <https://doi.org/10.1016/j.watres.2020.116738>, 2021.
- 695 Liu S., Kuhn, C., Amatulli, G., Aho, K., Butman, D.E., Allen, G.H., Lin, P., Pan, M., Yamazaki, D.,
696 Brinkerhoff, C., Gleason, C., Xia, X., and Raymond, P.A.: The importance of hydrology in routing
697 terrestrial carbon to the atmosphere via global streams and rivers, *PNAS* 119 No. 11, e2106322119;
698 <https://doi.org/10.1073/pnas.2106322119>, 2022.
- 699 Lobbes, J. M., Fitznar, H. P., and Kattner, G.: Biogeochemical characteristics of dissolved and particulate
700 organic matter in Russian rivers entering the Arctic Ocean, *Geochim. Cosmochim. Acta*, 64, 2973–
701 2983, [https://doi.org/10.1016/S0016-7037\(00\)00409-9](https://doi.org/10.1016/S0016-7037(00)00409-9), 2000.
- 702 Lundin, E. J., Giesler, R., Persson, A., Thompson, M. S., and Karlsson, J.: Integrating carbon emissions from
703 lakes and streams in a subarctic catchment, *J. Geophys. Res. Biogeosciences*, 118, 1200–1207,
704 <https://doi.org/10.1002/jgrg.20092>, 2013.
- 705 Lynch, L. M., Sutfin, N. A., Feghel, T. S., Boot, C. M., Covino, T. P., and Wallenstein, M. D.: River channel
706 connectivity shifts metabolite composition and dissolved organic matter chemistry, *Nat. Commun.*, 10,
707 459, <https://doi.org/10.1038/s41467-019-08406-8>, 2019.
- 708 Marie, D., Partensky, F., Vaultot, D., and Brussaard, C.: Enumeration of Phytoplankton, Bacteria, and Viruses
709 in Marine Samples, *Curr. Protoc. Cytom.*, 10, 11111–11115,
710 <https://doi.org/10.1002/0471142956.cy1111s10>, 1999.
- 711 Pekel, J.-F., Cottam, A., Gorelick, N., and Belward, A. S.: High-resolution mapping of global surface water
712 and its long-term changes, *Nature*, 540, 418–422, <https://doi.org/10.1038/nature20584>, 2016.
- 713 Pokrovsky, O. S., Manasypov, R. M., Loiko, S., Shirokova, L. S., Krickov, I. A., Pokrovsky, B. G.,
714 Kolesnichenko, L. G., Kopysov, S. G., Zemtsov, V. A., Kulizhsky, S. P., Vorobyev, S. N., and Kirpotin,
715 S. N.: Permafrost coverage, watershed area and season control of dissolved carbon and major elements



- 716 in western Siberian rivers, *Biogeosciences*, 12, 6301–6320, <https://doi.org/10.5194/bg-12-6301-2015>,
717 2015.
- 718 Pokrovsky, O. S., Manasyrov, R. M., Kopysov, S. G., Krickov, I. V., Shirokova, L. S., Loiko, S. V., Lim, A.
719 G., Kolesnichenko, L. G., Vorobyev, S. N., and Kirpotin, S. N.: Impact of permafrost thaw and climate
720 warming on riverine export fluxes of carbon, nutrients and metals in Western Siberia, *Water (MDPI)*,
721 12, 1817, <https://doi.org/10.3390/w12061817>, 2020.
- 722 Ran, L., Lu, X. X., Richey, J. E., Sun, H., Han, J., Yu, R., Liao, S., and Yi, Q.: Long-term spatial and temporal
723 variation of CO₂ partial pressure in the Yellow River, China, *Biogeosciences*, 12, 921–932,
724 <https://doi.org/10.5194/bg-12-921-2015>, 2015.
- 725 Ran, L., Lu, X. X., and Liu, S.: Dynamics of riverine CO₂ in the Yangtze River fluvial network and their
726 implications for carbon evasion, *Biogeosciences*, 14, 2183–2198, [https://doi.org/10.5194/bg-14-2183-](https://doi.org/10.5194/bg-14-2183-2017)
727 2017, 2017.
- 728 Raymond, P. A., McClelland, J. W., Holmes, R. M., Zhulidov, A. V., Mull, K., Peterson, B. J., Striegl, R. G.,
729 Aiken, G. R., and Gurtovaya, T. Y.: Flux and age of dissolved organic carbon exported to the Arctic
730 Ocean: A carbon isotopic study of the five largest arctic rivers, *Glob. Biogeochem. Cycles*, 21, GB4011,
731 <https://doi.org/10.1029/2007GB002934>, 2007.
- 732 Raymond, P. A., Hartmann, J., Lauerwald, R., Sobek, S., McDonald, C., Hoover, M., Butman, D., Striegl,
733 R., Mayorga, E., Humborg, C., Kortelainen, P., Dürr, H., Meybeck, M., Ciais, P., and Guth, P.: Global
734 carbon dioxide emissions from inland waters, *Nature*, 503, 355–359,
735 <https://doi.org/10.1038/nature12760>, 2013.
- 736 Rocher-Ros, G., Sponseller, R. A., Lidberg, W., Mörth, C.-M., and Giesler, R.: Landscape process domains
737 drive patterns of CO₂ evasion from river networks, *Limnol. Oceanogr. Lett.*, 4, 87–95,
738 <https://doi.org/10.1002/lol2.10108>, 2019.
- 739 Santoro, M., Beer, C., Cartus, O., Schullius, C., Shvidenko, A., McCallum, I., Wegmüller, U., and
740 Wiesmann, A.: The BIOMASAR algorithm: An approach for retrieval of forest growing stock volume
741 using stacks of multi-temporal SAR data, in: Proceedings of ESA Living Planet Symposium, Bergen,
742 Norway, 28 June – 2 July, 2010.
- 743 Semiletov, I. P., Pipko, I. I., Shakhova, N. E., Dudarev, O. V., Pugach, S. P., Charkin, A. N., McRoy, C. P.,
744 Kosmach, D., and Gustafsson, Ö.: Carbon transport by the Lena River from its headwaters to the Arctic
745 Ocean, with emphasis on fluvial input of terrestrial particulate organic carbon vs. carbon transport by
746 coastal erosion, *Biogeosciences*, 8, 2407–2426, <https://doi.org/10.5194/bg-8-2407-2011>, 2011.
- 747 Serikova, S., Pokrovsky, O. S., Ala-Aho, P., Kazantsev, V., Kirpotin, S. N., Kopysov, S. G., Krickov, I. V.,
748 Laudon, H., Manasyrov, R. M., Shirokova, L. S., Soulsby, C., Tetzlaff, D., and Karlsson, J.: High
749 riverine CO₂ emissions at the permafrost boundary of Western Siberia, *Nat. Geosci.*, 11, 825–829,
750 <https://doi.org/10.1038/s41561-018-0218-1>, 2018.
- 751 Serikova, S., Pokrovsky, O. S., Laudon, H., Krickov, I. V., Lim, A. G., Manasyrov, R. M., and Karlsson, J.:
752 High carbon emissions from thermokarst lakes of Western Siberia, *Nat. Commun.*, 10,
753 <https://doi.org/10.1038/s41467-019-09592-1>, 2019.
- 754 Stackpoole, S. M., Butman, D. E., Clow, D. W., Verdin, K. L., Gaglioti, B. V., Genet, H., and Striegl, R. G.:
755 Inland waters and their role in the carbon cycle of Alaska, *Ecol. Appl.*, 27, 1403–1420,
756 <https://doi.org/10.1002/eap.1552>, 2017.
- 757 Striegl, R. G., Dornblaser, M. M., McDonald, C. P., Rover, J. A., and Stets, E. G.: Carbon dioxide and
758 methane emissions from the Yukon River system, *Glob. Biogeochem. Cycles*, 26, GB0E05,
759 <https://doi.org/10.1029/2012GB004306>, 2012.
- 760 Teodoru, C. R., del Giorgio, P. A., Prairie, Y. T., and Camire, M.: Patterns in pCO₂ in boreal streams and
761 rivers of northern Quebec, Canada, *Glob. Biogeochem. Cycles*, 23, GB2012,
762 <https://doi.org/10.1029/2008GB003404>, 2009.
- 763 Tranvik, L., Cole, J. J., and Prairie, Y. T.: The study of carbon in inland waters—from isolated ecosystems to
764 players in the global carbon cycle, *Limnol. Oceanogr. Lett.*, 3, 41–48,
765 <https://doi.org/10.1002/lol2.10068>, 2018.
- 766 Turetsky, M.R., Abbott, B.W., Jones, M.C., Anthony, K.W., Olefeldt, D., Schuur, E.A.G., Grosse, G., Kuhry,
767 P., Hugelius, G., Koven, C., et al. : Carbon release through abrupt permafrost thaw, *Nat. Geoscience*,
768 13, 138–143, doi:10.1038/s41561-019-0526-0, 2020.



- 769 Vachon, D., Sponseller, R. A., and Karlsson, J.: Integrating carbon emission, accumulation and transport in
770 inland waters to understand their role in the global carbon cycle, *Glob. Change Biol.*, 27, 719–727,
771 <https://doi.org/10.1111/gcb.15448>, 2021.
- 772 Vorobyev, S. N., Pokrovsky, O. S., Kolesnichenko, L. G., Manasyrov, R. M., Shirokova, L. S., Karlsson, J.,
773 and Kirpotin, S. N.: Biogeochemistry of dissolved carbon, major, and trace elements during spring flood
774 periods on the Ob River, *Hydrol. Process.*, 33, 1579–1594, <https://doi.org/10.1002/hyp.13424>, 2019.
- 775 Vorobyev, S. N., Karlsson, J., Kolesnichenko, Y. Y., Korets, M. A., and Pokrovsky, O. S.: Fluvial carbon
776 dioxide emission from the Lena River basin during the spring flood, *Biogeosciences*, 18, 4919–4936,
777 <https://doi.org/10.5194/bg-18-4919-2021>, 2021.
- 778 Wallin, M. B., Öquist, M. G., Buffam, I., Billett, M. F., Nisell, J., and Bishop, K. H.: Spatiotemporal
779 variability of the gas transfer coefficient (K_{CO_2}) in boreal streams: Implications for large scale
780 estimates of CO_2 evasion, *Glob. Biogeochem. Cycles*, 25, GB3025,
781 <https://doi.org/10.1029/2010GB003975>, 2011.
- 782 Wallin, M. B., Grabs, T., Buffam, I., Laudon, H., Ågren, A., Öquist, M. G., and Bishop, K.: Evasion of CO_2
783 from streams – The dominant component of the carbon export through the aquatic conduit in a boreal
784 landscape, *Glob. Change Biol.*, 19, 785–797, <https://doi.org/10.1111/gcb.12083>, 2013.
- 785 Wallin, M. B., Campeau, A., Audet, J., Bastviken, D., Bishop, K., Kokic, J., Laudon, H., Lundin, E., Löfgren,
786 S., Natchimuthu, S., Sobek, S., Teutschbein, C., Weyhenmeyer, G. A., and Grabs, T.: Carbon dioxide
787 and methane emissions of Swedish low-order streams—a national estimate and lessons learnt from
788 more than a decade of observations, *Limnol. Oceanogr. Lett.*, 3, 156–167,
789 <https://doi.org/10.1002/lol2.10061>, 2018.
- 790 Wanninkhof, R.: Relationship between wind speed and gas exchange over the ocean, *J. Geophys. Res.*
791 *Oceans*, 97, 7373–7382, <https://doi.org/10.1029/92JC00188>, 1992.
- 792 Wild, B., Andersson, A., Bröder, L., Vonk, J., Hugelius, G., McClelland, J. W., Song, W., Raymond, P. A.,
793 and Gustafsson, Ö.: Rivers across the Siberian Arctic unearth the patterns of carbon release from
794 thawing permafrost, *PNAS*, 116, 10280–10285, <https://doi.org/10.1073/pnas.1811797116>, 2019.
- 795 Winterdahl, M., Wallin, M. B., Karlson, R. H., Laudon, H., Öquist, M., and Lyon, S. W.: Decoupling of
796 carbon dioxide and dissolved organic carbon in boreal headwater streams, *J. Geophys. Res.*
797 *Biogeosciences*, 121, 2630–2651, <https://doi.org/10.1002/2016JG003420>, 2016.
- 798 Zolkos, S., Tank, S. E., Striegl, R. G., and Kokelj, S. V.: Thermokarst effects on carbon dioxide and methane
799 fluxes in streams on the Peel Plateau (NWT, Canada), *J. Geophys. Res. Biogeosciences*, 124, 1781–
800 1798, <https://doi.org/10.1029/2019JG005038>, 2019.

801

802

803

804

805

806

807

808

809

810

811

812

813

814



815

816 **Table 1.** Measured hydrochemical and GHG exchange parameters in the Ket River main stem and
817 tributaries (average ± s.d.; (n) is number of measurements).

818

819

Parameter	unit	Tributaries		Main stem	
		Flood (n=26)	Base flow (n=12)	Flood (n=7)	Base flow (n=6)
Water temperature	°C	9.48±2.25	14.9±1.24	9.06±1.59	16.5±0.54
pH		6.31±0.45	6.71±0.57	6.2±0.43	7.29±0.26
Dissolved O ₂	mg L ⁻¹	8.53±1.26	8.02±1.13	8.85±0.83	8.78±0.18
Specific Conductivity	µS cm ⁻¹	40.7±22.7	126.9±62.1	39±14.9	181±36.8
DIC	mg L ⁻¹	2.83±2.58	17.8±10.4	2.43±1.49	20.5±5.22
DOC	mg L ⁻¹	21.7±3.94	15.7±7.04	21.9±4.28	16.6±3.57
SUVA ₂₅₄	L mg C ⁻¹ m ⁻¹	4.34±0.33	4.9±0.66	4.29±0.18	4.26±0.52
PON	mg L ⁻¹	0.08±0.06	0.64±0.27	0.1±0.07	0.96±0.22
POC	mg L ⁻¹	2.41±1.17	8±2.36	2.55±1.2	9.49±1.98
TBC	*10 ⁵ cells ml ⁻¹	5.89±3.26	8.69±3.21	5.95±2.83	4.94±2.15
K _T	m d ⁻¹	0.53±0.38	1.21±0.52	0.77±0.55	1.22±0.37
FCO ₂	g C m ⁻² d ⁻¹	1.3±0.76	2.63±2.15	1.35±1.08	1.16±0.5
pCO ₂	µatm	2877±679	4005±1494	2405±328	2523±981
FCH ₄	mmol C m ⁻² d ⁻¹	0.39±0.95	1.38±1.21	0.06±0.05	0.95±0.88
CH ₄	µmol L ⁻¹	0.65±0.66	1.17±0.81	0.17±0.01	0.86±0.91

820

821

822

823

824

825

826

827

828

829

830

831

832

833

834

835

836

837

838

839

840

841

842

843

844

845

846



847 **Table 2.** Pearson correlation coefficients of measured FCO₂, CO₂, and CH₄ concentration with
 848 hydrochemical parameters of the water column (DOC, SUVA, particulate organic carbon and nitrogen, total
 849 bacterial cells) and landscape parameters of the tributaries and the main stem of the Ket River. Significant
 850 (p < 0.05) values are labeled by asterisk.
 851

	all seasons			flood			baseflow		
	CH ₄	CO ₂	FCO ₂	CH ₄	CO ₂	FCO ₂	CH ₄	CO ₂	FCO ₂
Hydrochemical parameters									
pH	0.2	-0.1	-0.2	-0.1	0.1	-0.2	0.0	-0.6*	-0.6*
Dissolved O ₂	-0.1	-0.7*	-0.1	0.0	-0.8*	0.1	-0.2	-0.8*	-0.7*
Specific conductivity	0.3	0.0	0.1	-0.2	0.0	0.1	0.2	-0.3	-0.6*
DIC	0.3	0.0	0.0	-0.1	0.0	0.1	0.2	-0.4	-0.7*
DOC	-0.1	0.0	0.1	0.3	0.0	-0.1	-0.2	-0.1	0.2
SUVA ₂₅₄	0.1	0.2	0.3	0.4	-0.3	0.1	-0.2	0.5*	0.6*
PON	0.1	-0.1	0.2	-0.2	-0.4*	0.2	-0.4	-0.5*	-0.5
POC	0.1	-0.1	0.2	-0.2	-0.4*	0.1	-0.3	-0.3	0.1
TBC	0.2	0.2	0.1	0.3	-0.2	-0.1	0.0	0.5*	0.5*
Climatic characteristics									
MAAT	0.2	0.0	-0.5*	0.1	0.0	-0.4*	0.2	0.1	-0.5
MAP	0.0	0.3*	0.5*	0.1	0.0	0.3	0.1	0.6*	0.7*
Land-cover characteristics									
Watershed area	-0.3	-0.3*	0.2	-0.4	-0.5*	0.0	-0.2	-0.1	0.5
Dark Needleleaf Forest	0.1	0.0	-0.3	0.1	0.0	-0.3	0.2	-0.1	-0.2
Light Needleleaf Forest	0.3*	0.4*	0.2	0.4	0.2	0.0	0.4	0.7*	0.6*
Broadleaf Forest	-0.3	-0.4*	0.1	-0.5*	-0.4	0.1	-0.3	-0.6*	-0.2
Mixed Forest	0.0	-0.2	-0.3	0.1	-0.1	-0.3	-0.1	-0.4	-0.4
Peatlands and bogs	0.0	0.2	0.3	-0.1	0.0	0.2	0.1	0.2	0.4
Riparian Vegetation	-0.1	0.0	-0.1	-0.2	0.1	0.0	-0.2	-0.2	-0.5
Grassland	0.1	-0.1	0.0	-0.1	-0.2	0.1	0.3	0.0	-0.5
Recent Burns	-0.1	-0.1	0.2	-0.1	-0.2	0.1	-0.3	0.1	0.4
Water Bodies	-0.2	-0.1	0.3	-0.3	-0.3	0.2	-0.2	-0.1	0.3
Lithology characteristics									
Upper Cretaceous, Maastrichtian – (sedimentary, silicate)	0.1	-0.4*	0.0	0.3	-0.3	0.2	0.0	-0.5*	-0.4
Lower Paleocene (sedimentary silicate rocks)									
Paleogene. Upper Oligocene (clays and silts)	0.1	-0.2	0.1	0.1	-0.1	0.2	0.0	-0.5*	-0.2
Cretaceous. Coniacian – Campanian (carbonates)	-0.2	-0.4*	-0.3	-0.2	-0.2	-0.2	-0.3	-0.7*	-0.6*
Neogene. Lower -Middle Miocene (clays, silts)	-0.1	0.2	0.3	-0.1	0.0	0.2	-0.1	0.3	0.3
Upper Pliocene-Eopleistocene (sands)	0.0	0.2	0.1	0.0	0.2	0.0	0.0	0.3	0.3
Cretaceous. Cenoman – Turon (clays, some carbonates)	-0.2	-0.5*	-0.3	-0.3	-0.3	-0.2	-0.3	-0.7*	-0.6*
Neogene. Lower Miocene (sands)	0.1	-0.2	-0.1		-0.2	-0.2	0.1	-0.3	0.0

852

853

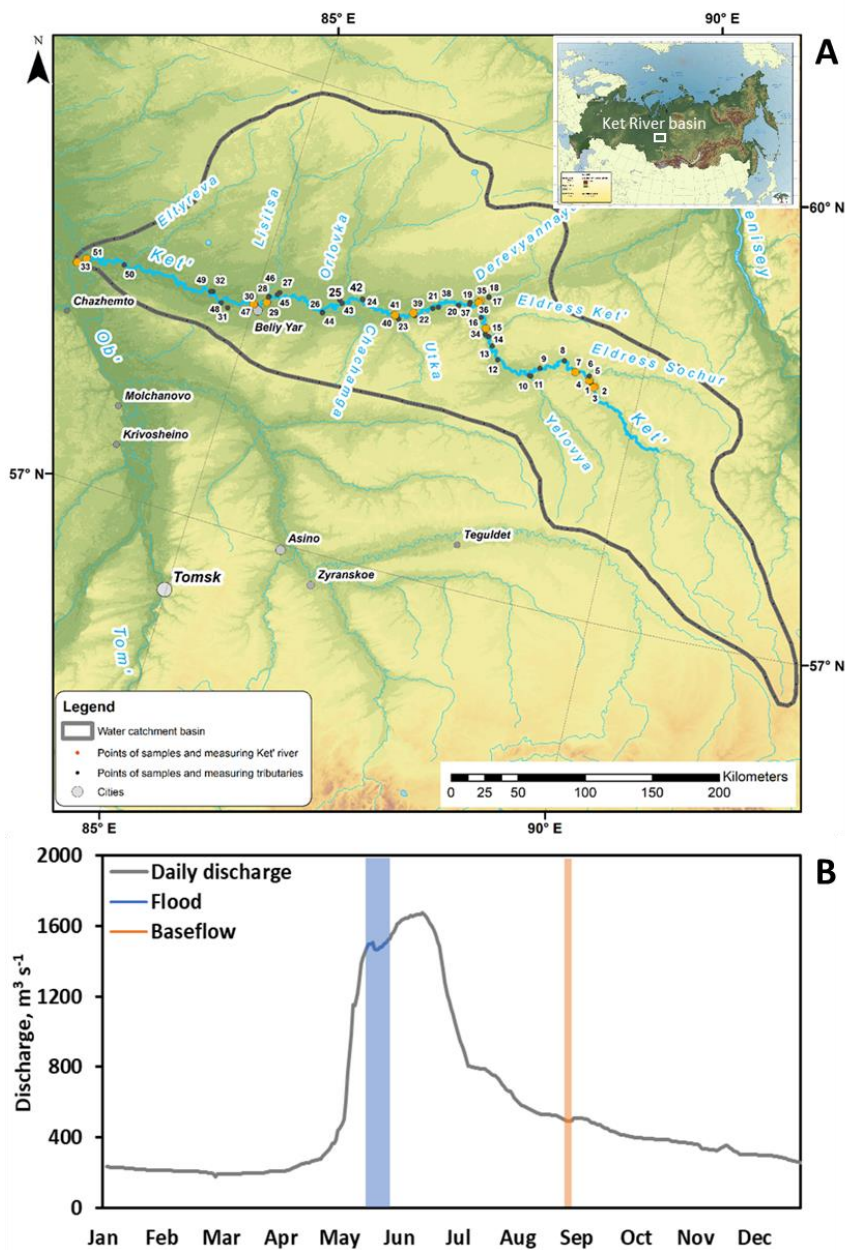
854

855

856

857

858



859

860

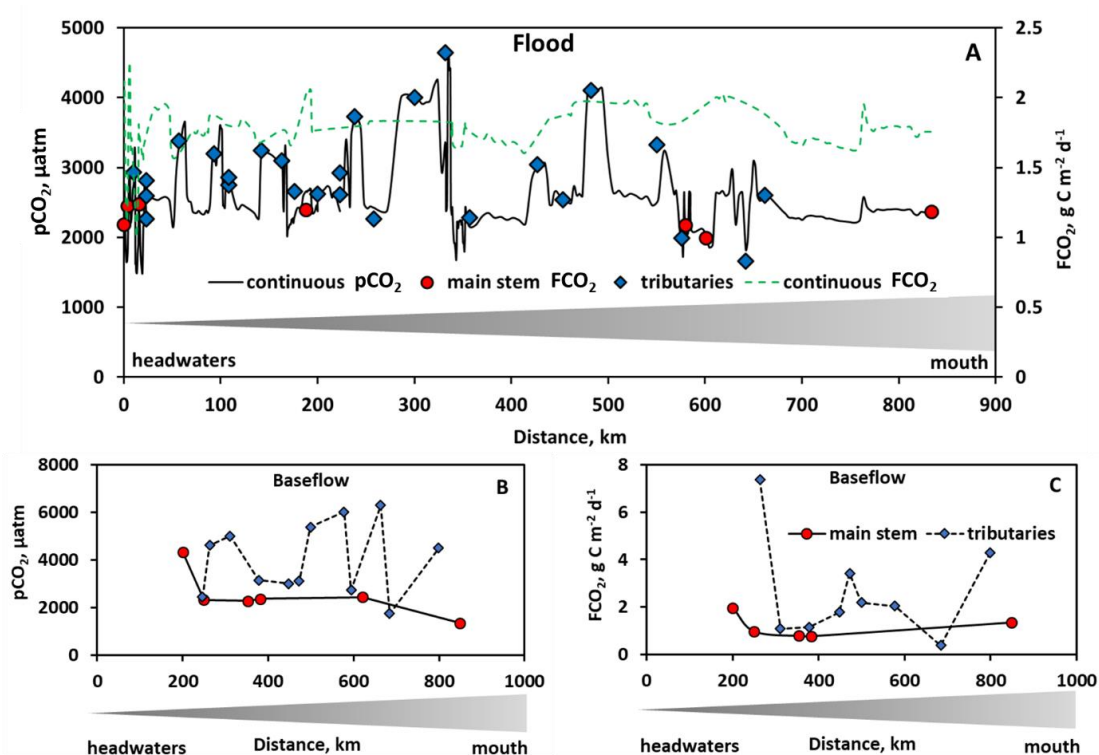
861 **Fig. 1. A:** Map of the studied Ket River watershed with continuous pCO₂ measurements in the main stem.

862 **B:** Daily discharge (Q) at the gauging station of the Ket mouth, Rodionovka, in 2019. Highlighted in blue

863 and orange are two sampling campaigns of this study, spring flood and summer-autumn baseflow.

864

865



866

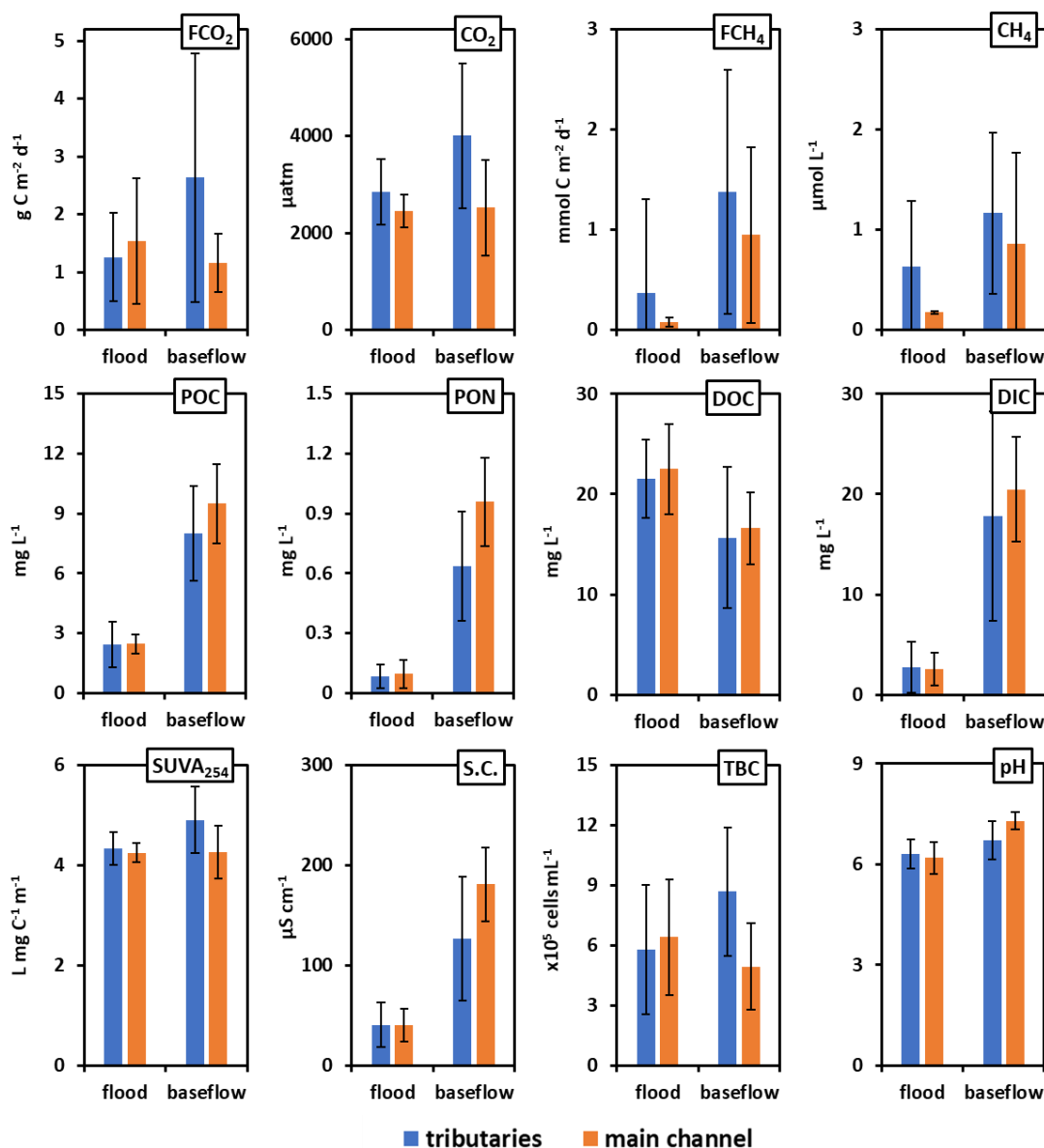
867

868

869 **Figure 2.** The pCO₂ and measured and calculated CO₂ fluxes during spring (A) and summer (B, C) of the
 870 Ket River main stem and tributaries (over the 830 km distance, from the headwaters to the mouth (left to
 871 right). Continuous CO₂ measurements in (A) are only for the main stem. Note that during summer baseflow,
 872 the water level did not allow reaching the headwaters of the Ket River (first 0-200 km on the river course).

873

874



875

876

877

878 **Figure 3.** Mean (\pm s.d.) GHG concentration and fluxes, hydrochemical parameters, particulate organic
 879 carbon and nitrogen (POC and PON, respectively) and total bacteria count (TBC), in the main channel
 880 (orange column) and the tributaries (blue column) of the Ket River in spring flood and summer (early fall)
 881 baseflow.

882

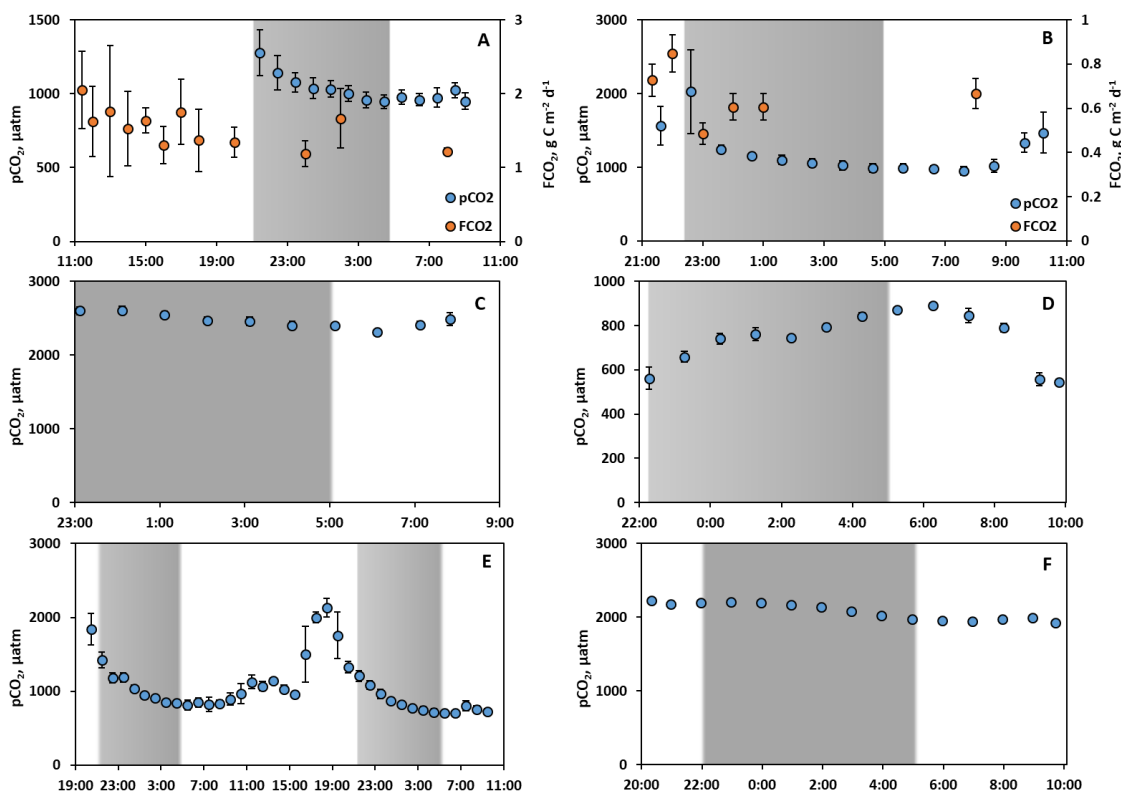
883

884



885

886



887
888

889

890

891 **Figure 4.** Continuous pCO₂ concentration (A-F, blue circles) and chamber-based fluxes (A, B) measured
 892 during spring flood period in tributaries (A Sochur No 3, B Lopatka No 8, C Derevyannaya No 12, D Ob
 893 river entrance, E Segondenka No 26) and in the Ket River main stem (middle course) near Stepanovka
 894 village (F) including night time measurements (shaded area). Variations of water temperature were within
 895 the range of 0.3 to 0.6 °C and did not exhibit significant correlations with pCO₂ and FCO₂.

896

897

898

899

900

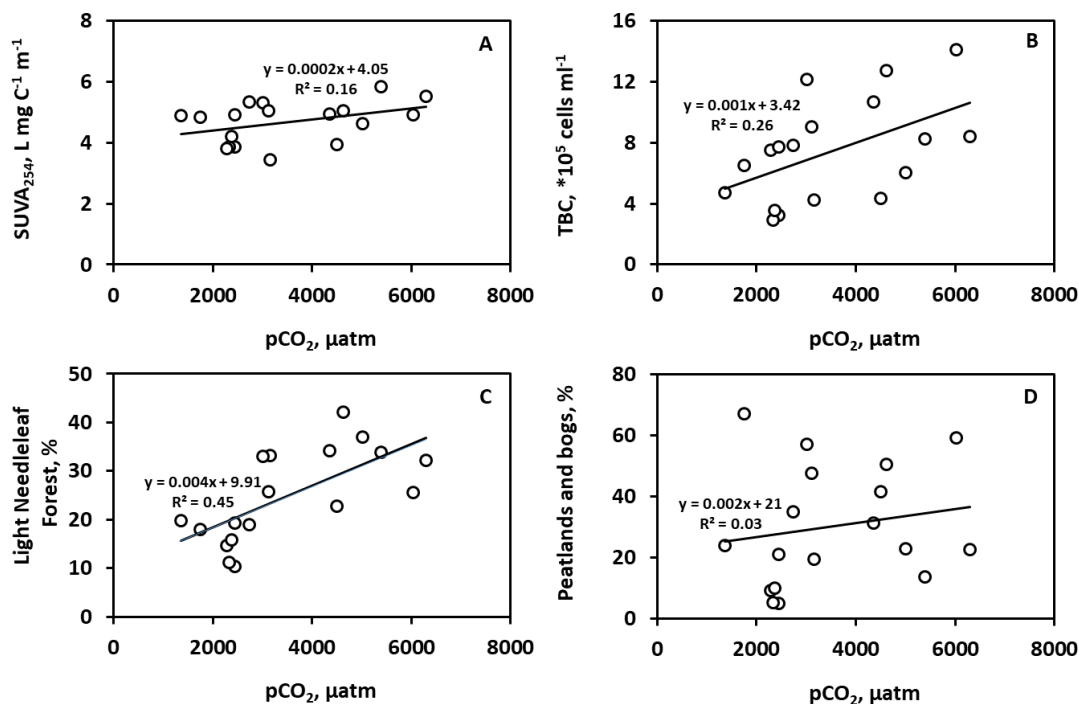
901

902

903



904



905

906

907

908 **Figure 5.** Significant ($p < 0.05$) positive control of SUVA (A), Total Bacterial Count (B), Light needleleaf
909 forest (C) and wetlands (D) on CO₂ concentration in the Ket River and tributaries during summer baseflow.

910

911

912

913

914

915

916

917

918

919

920

921